Chaos and Ergodicity across the Energy Spectrum of Interacting Bosons

Lukas Pausch,[1] Edoardo G. Carnio,[1,2] Alberto Rodríguez,[3,*] and Andreas Buchleitner[1,2,†]
[1]Physikalisches Institut, Albert-Ludwigs-Universität Freiburg, Hermann-Herder-Straße 3, D-79104 Freiburg, Germany
[2]EUCOR Centre for Quantum Science and Quantum Computing, Albert-Ludwigs-Universität Freiburg, Hermann-Herder-Straße 3, D-79104 Freiburg, Germany
[3]Departamento de Física Fundamental, Universidad de Salamanca, E-37008 Salamanca, Spain

(Received 10 September 2020; revised 20 January 2021; accepted 24 February 2021; published 12 April 2021)

We identify the chaotic phase of the Bose-Hubbard Hamiltonian by the energy-resolved correlation between spectral features and structural changes of the associated eigenstates as exposed by their generalized fractal dimensions. The eigenvectors are shown to become ergodic in the thermodynamic limit, in the configuration space Fock basis, in which random matrix theory offers a remarkable description of their typical structure. The distributions of the generalized fractal dimensions, however, are ever more distinguishable from random matrix theory as the Hilbert space dimension grows.

DOI: 10.1103/PhysRevLett.126.150601

Ergodicity, understood as the ability of a system to dynamically explore, irrespective of its initial state, all possible configurations at given energy, is, in general, an exceedingly difficult to prove and rather rare property, at the classical and quantum level [1–3]. On the quantum side, safe ground is established by (intrinsically ergodic [4]) random matrix theory (RMT), which describes systems with classically strictly chaotic ("K-systems" [1–3,5]) dynamics [6]. RMT predictions for energy spectra and eigenstates [7,8] define popular benchmarks to certify ergodicity [9,10].

Ergodicity can, however, emerge on widely variable time scales, hinging on finer structures of phase space, and, at the quantum level, on the effective coarse graining thereof induced by the finite size of $\hbar$ [11]. Since the majority of dynamical systems features mixed rather than strictly chaotic dynamics [12–17], one therefore expects detectable deviations from RMT ergodicity [18,19], in particular at the level of the eigenvectors' structural properties—which reflect the underlying phase space structure [12–16,20]. This holds on the level of single as well as of many-body quantum systems, with engineered ensembles of ultracold atoms [21–26] as a modern playground: Notably, interacting bosons on a regular lattice provide a paradigmatic experimental setting to explore the questions above [27–31]; they feature chaos on the level of spectral [32–35] and eigenvector properties [32,33,36–39] as well as quench dynamics [40–44].

Here we consider the one-dimensional Bose-Hubbard Hamiltonian (BHH) and combine state-of-the-art numerical simulations with analytical calculations to establish a so far missing integral picture of its chaotic and nonergodic phases, providing deeper insight into the concept of chaos and ergodicity in the quantum realm. We demonstrate that (i) the energy-resolved chaotic phase is signaled by a clear correlation between spectral features and eigenstate structural changes captured by generalized fractal dimensions (GFDs) (cf. Fig. 1), whose fluctuations exhibit the same qualitative behavior in the two natural bases of the Hamiltonian, (ii) a nonergodic phase persists in the thermodynamic limit, as a function of a scaled tunneling strength, (iii) eigenvectors within the chaotic phase become ergodic in the thermodynamic limit in the configuration space Fock basis, where RMT provides a remarkable description of the eigenstates' typical (i.e., most probable) GFDs, (iv) despite such agreement, according to the GFD distributions BHH and RMT depart from each other in an unequivocal statistical sense with increasing size of Hilbert space. This implies that the fluctuations of the eigenstates' structure along the path to ergodicity (even if it be arbitrarily close to RMT at a coarse-grained level) contain statistically robust fingerprints of the specific underlying Hamiltonian.

In terms of standard bosonic operators associated with L Wannier spatial modes, the BHH [45–47] is the sum of a tunneling and a local interaction Hamiltonian with respective strengths J and U,

$$H_{\mathrm{tun}} = -J\sum_{k}(b_k^\dagger b_{k+1} + b_{k+1}^\dagger b_k), \tag{1}$$

$$H_{\mathrm{int}} = \frac{U}{2}\sum_{k} n_k(n_k - 1). \tag{2}$$

The BHH exhibits a Z_2 symmetry under the reflection operation (Π) about the center of the lattice. In the presence of periodic boundary conditions (PBCs), the BHH additionally has translational symmetry, and Hilbert space can be decomposed into L irreducible blocks distinguished by the center-of-mass quasimomentum Q. The $Q = 0$ block

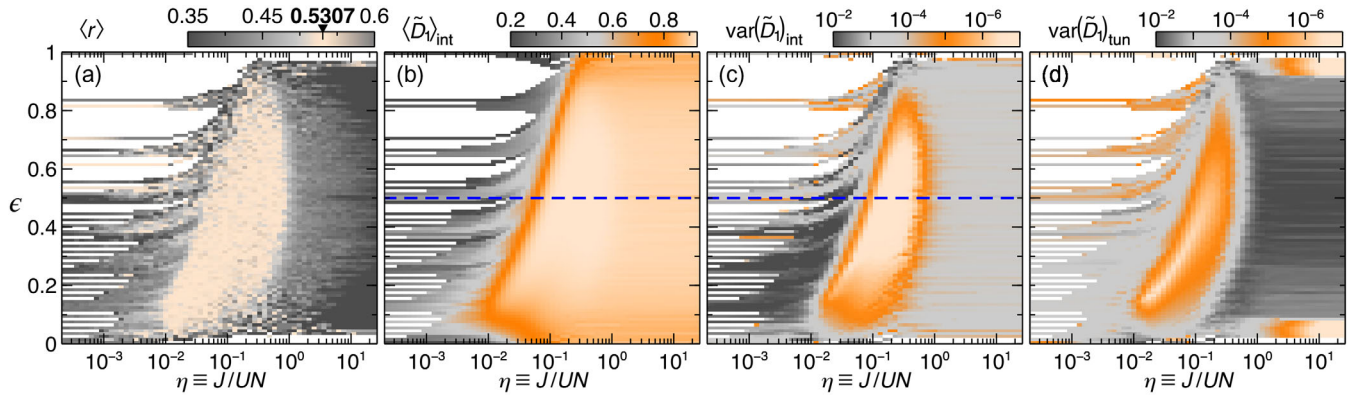

FIG. 1. Evolution of $\langle r\rangle$ (a), $\langle\tilde{D}_1\rangle$ in the eigenbasis of $H_{\rm int}$ (b) and $\mathrm{var}(\tilde{D}_1)$ in the eigenbases of $H_{\rm int}$ (c) and $H_{\rm tun}$ (d), as functions of η and energy $\epsilon = (E - E_{\rm min})/(E_{\rm max} - E_{\rm min})$, for the irreducible Hilbert subspace of size $\mathcal{N} = 55898$ with $Q = 0$ and $\pi = -1$, for $N = L = 12$ with PBCs. The spectrum was obtained for 75 equally spaced values of $\log_{10}(J/U) \in [-2.92, 3]$, and divided into 100 bins of equal width along the ϵ axis. The value $\langle r\rangle_{\rm GOE}$ is highlighted over the left color bar. Blue dashed lines mark the value $\epsilon = 0.5$ considered in Fig. 2.

further disjoins into symmetric ($\pi = +1$) and antisymmetric ($\pi = -1$) subspaces. For hard-wall boundary conditions (HWBCs), the latter π division applies to the full Hilbert space.

Both $H_{\rm tun}$ and $H_{\rm int}$ are integrable and analytically solvable in appropriate Fock bases. The eigenvectors of the interaction term are the Fock states of the on-site number operators, $|\mathbf{n}\rangle \equiv |n_1, \ldots, n_L\rangle$, with $||\mathbf{n}||_1 = N$, where N is the number of bosons. The eigenvectors of $H_{\rm tun}$ follow from the Fock states of number operators of spatially delocalized plane-wave or standing-wave modes, for PBCs or HWBCs, respectively.

The competition between tunneling and interaction makes the BHH nonintegrable: For comparable J and U, it exhibits spectral chaos [32–35], identified by short-range spectral measures in accord with the Gaussian orthogonal ensemble (GOE) of RMT. This may be traced back to the underlying classical Hamiltonian [16,34,48], whose dynamics are governed by the scaled energy H/UN^2 and the scaled tunneling strength $\eta \equiv J/UN$. In the quantum system, one therefore expects η to control the emergence of chaos in sufficiently dense spectral regions.

We numerically analyze the BHH at unit filling ($N = L$): Eigenstates around chosen energy targets [49–51] as well as full spectra, scaled as $\epsilon \equiv (E - E_{\rm min})/(E_{\rm max} - E_{\rm min}) \in [0, 1]$, enabling the juxtaposition of results for different N and η, are obtained by exact diagonalization. Since the form of $H_{\rm tun}$ and $H_{\rm int}$ reveals that $E_{\rm max} - E_{\rm min} \sim UN^2$ for large N, ϵ effectively provides the classically scaled energy. Short-range statistical features of the spectrum are best captured by the level spacing ratios [52,53], $r_n = \min(s_{n+1}/s_n, s_n/s_{n+1})$, where $s_n = E_{n+1} - E_n$ is the nth level spacing. The distributions of r are known approximately analytically for Gaussian random matrix ensembles and accessible numerically without further unfolding procedures, e.g., $\langle r\rangle_{\rm GOE} \approx 0.5307$ [53].

The eigenstate structure of generic many-body Hamiltonians in Hilbert space exhibits multifractal complexity [54–64], and is conveniently described by finite-size generalized fractal dimensions (GFDs) [62,65],

$$\tilde{D}_q \equiv \frac{1}{1-q}\log_{\mathcal{N}} R_q, \quad \text{with} \quad R_q = \sum_\alpha |\psi_\alpha|^{2q}, q \in \mathbb{R}^+, \tag{3}$$

for eigenvectors with amplitudes ψ_α in a given orthonormal basis of size $\mathcal{N}$. The eigenvector moments are expected to scale asymptotically as $R_q \sim \mathcal{N}^{-(q-1)D_q}$, where the dimensions $D_q \equiv \lim_{\mathcal{N}\to\infty} \tilde{D}_q$ decide whether the state is localized ($D_q = 0$ for $q \geq 1$ [66]), multifractal (extended nonergodic; q-dependent $0 < D_q < 1$), or ergodic ($D_q = 1$ for all q), in the chosen expansion basis. Consequently, the support of ergodic eigenstates—e.g., the eigenvectors of the Wigner-Dyson RMT ensembles [68]—scales asymptotically as the full Hilbert space. Among all GFDs, we focus on $\tilde{D}_1$, governing the scaling of the Shannon entropy of $\{|\psi_\alpha|^2\}$, $\tilde{D}_2$, determining the scaling of the eigenstate's inverse participation ratio, and $\tilde{D}_\infty = -\log_{\mathcal{N}} \max_\alpha |\psi_\alpha|^2$, unveiling the extreme statistics of the state's intensities.

We first analyze the connection between spectral chaos and the eigenstates' GFDs. In Figs. 1(a)–1(c), we show the evolution of $\langle r\rangle$, $\langle\tilde{D}_1\rangle$, and $\mathrm{var}(\tilde{D}_1)$, as functions of scaled energy ϵ and scaled tunneling strength η, for $N = 12$ and PBCs (subspace $Q = 0$, $\pi = -1$), evaluated in the eigenbasis of $H_{\rm int}$. The ϵ spectrum is divided into 100 bins of equal width; mean values and variances are computed from eigenvalues and eigenvectors falling into each bin. Energy-resolved density plots expose the coarse-grained level dynamics of the system: Heavily degenerate manifolds of $H_{\rm int}$ fan out as η increases, overlap, and then form a bulk region massively populated by avoided crossings (observable upon finer inspection [69]), which eventually dissolves

as the levels reorganize into the bands allowed by $H_{\rm tun}$, for $\eta \gg 1$. We identify a slightly bent oval region of spectral chaos, centered around $\eta \simeq 0.1$ and extending over $0.1 \lesssim \epsilon \lesssim 0.9$, where $\langle r \rangle$ attains the GOE value. This region remains visible after averaging r over a large portion of the bulk spectrum, even without resolving the Π symmetry [70]. The onset of spectral chaos correlates with a sudden increase in the eigenvectors' GFDs, which reach maximum values within the spectral chaos region, as demonstrated for $\langle \tilde{D}_1 \rangle$. Strictly simultaneously, the energy-resolved GFD variance undergoes a dramatic reduction by several orders of magnitude. This behavior is also revealed by $\tilde{D}_2$ and $\tilde{D}_\infty$, and qualitatively the same in any irreducible subspace, also for HWBCs. The chaotic regime can therefore be identified by the unambiguous correlation between spectral features and structural changes of eigenstates, which, as revealed by the GFDs, tend to homogenize their delocalization in Hilbert space, irrespective of their energy.

To elucidate the eigenstates' structural dependence on the Hilbert space's size, Fig. 2 shows the mean and variance of $\tilde{D}_1$, for fixed $\epsilon = 0.5$ (where the density of states is maximum once spectral chaos kicks in), versus η, for increasing size (up to $\mathcal{N} \approx 2.6 \times 10^6$) of the $\pi = -1$ subspace with HWBCs. $\langle \tilde{D}_1 \rangle$ registers a surge around $\eta = 0.1$, and reaches a maximum that develops into a distinct plateau, extending towards larger η for increasing L. (Also $\langle r \rangle$ exhibits plateau broadening at $\epsilon = 0.5$ [69].) This behavior is mirrored by the drastic (ever bigger, with increasing L) drop of $\mathrm{var}(\tilde{D}_1)$, with plateaux at its minima. Note that the plateau values of $\langle \tilde{D}_1 \rangle$ and $\mathrm{var}(\tilde{D}_1)$ agree well with those expected for GOE eigenvectors, indicated by dashed lines in Fig. 2. The same is qualitatively observed for $q = 2, \infty$, other irreducible subspaces, and PBCs. The onset of the plateaux appears system size independent in terms of η [70], confirming the relevance of the classically scaled tunneling strength.

To shed further light on the GFD asymptotics within the chaotic region, the lower panels of Fig. 3 show $\langle \tilde{D}_q \rangle$ and $\mathrm{var}(\tilde{D}_q)$ at $\epsilon = 0.5$ and $\eta = 0.25$, for increasing $\mathcal{N}$ of four irreducible subspaces, evaluated in the corresponding eigenbases of $H_{\rm int}$. The results are compared against the GOE values, which, using known distributions [74] and extreme statistics [75], can be estimated analytically [70]. We find, asymptotically,

$$\langle \tilde{D}_1 \rangle_{\rm GOE} = 1 - \frac{1}{\ln \mathcal{N}} \left[2 - \gamma - \ln 2 - \frac{1}{\mathcal{N}} + O(\mathcal{N}^{-2}) \right], \quad (4)$$

$$\langle \tilde{D}_\infty \rangle_{\rm GOE} = 1 - \frac{\ln(2 \ln \mathcal{N})}{\ln \mathcal{N}} + O(\ln \ln \mathcal{N} / \ln^2 \mathcal{N}), \quad (5)$$

where γ is Euler's constant, and

$$\mathrm{var}(\tilde{D}_1)_{\rm GOE} = \frac{1}{\ln^2 \mathcal{N}} \left[\frac{3\pi^2 - 28}{2\mathcal{N}} + O(\mathcal{N}^{-2}) \right], \quad (6)$$

$$\mathrm{var}(\tilde{D}_\infty)_{\rm GOE} \sim \ln^{-4} \mathcal{N}. \quad (7)$$

For $q = 2$, we compare the results to the ensemble-averaged GFD, $\langle \tilde{D}_q^{(\rm ens)} \rangle_{\rm GOE} = \log_{\mathcal{N}} \langle R_q \rangle / (1 - q)$, instead [19,70], with finite-size corrections found identical (up to coefficients) with those for $\tilde{D}_1$. As shown in Fig. 3, the GFDs, as well as $\mathrm{var}(\tilde{D}_q)$, in the eigenbasis of $H_{\rm int}$ quickly approach GOE values, independently of subspace or

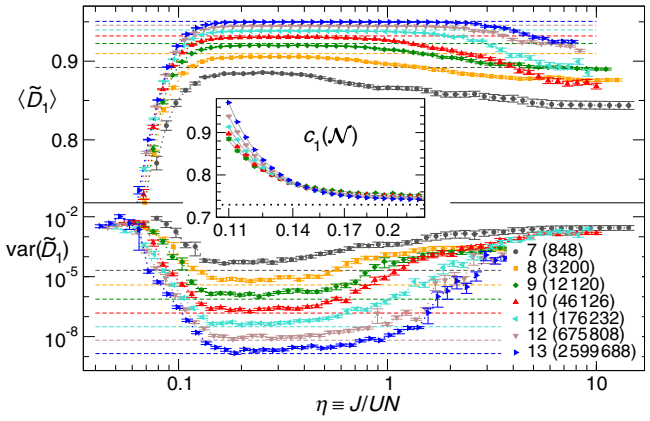

FIG. 2. Evolution of $\langle \tilde{D}_1 \rangle$ (top) and $\mathrm{var}(\tilde{D}_1)$ (bottom) at $\epsilon = 0.5$ versus η, for varying values of L and size ($\mathcal{N}$) (as indicated by the legend) of the subspace spanned by the $\pi = -1$ eigenstates of $H_{\rm int}$ with HWBCs. Each data point results from the analysis of the 100 BHH eigenvectors closest to $\epsilon = 0.5$. Corresponding GOE values are indicated by dashed lines. The inset shows the behavior of $c_1(\mathcal{N}) = (1 - \langle \tilde{D}_1 \rangle) \ln \mathcal{N}$ versus η around the crossover region (solid lines are guides to the eye). The horizontal dotted line marks the GOE value of $c_1(\mathcal{N} \to \infty)$.

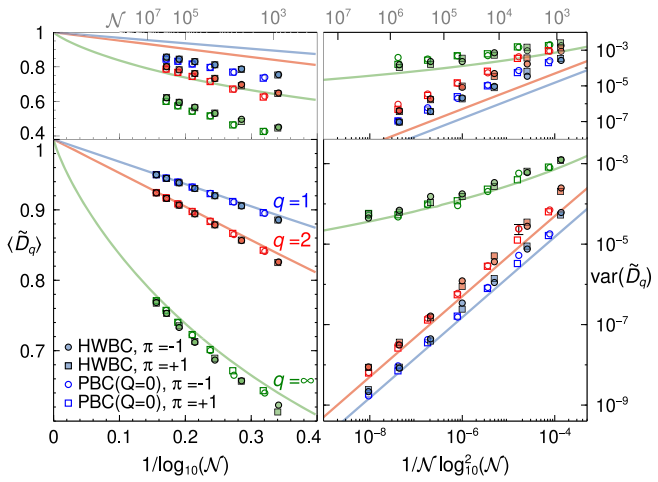

FIG. 3. Average and variance of $\tilde{D}_1$, $\tilde{D}_2$, and $\tilde{D}_\infty$, at $\eta = 0.25$ and $\epsilon = 0.5$, versus size $\mathcal{N}$ of four Hilbert subspaces (distinguished by symbols as indicated; each data point involves 100 eigenstates as in Fig. 2). Lower (upper) panels correspond to the analysis in the eigenbasis of $H_{\rm int}$ ($H_{\rm tun}$). Solid lines show GOE predictions. Whenever not shown, errors are contained within symbol size.

boundary conditions (for the largest $\mathcal{N}$ shown, $\langle \tilde{D}_1 \rangle_{\mathrm{GOE}} - \langle \tilde{D}_1 \rangle = 8 \times 10^{-4}$). The dominant finite-size correction seems to have the same $\mathcal{N}$ dependence for the BHH as for GOE eigenvectors, and the GFDs show clear evidence of converging to 1 in the thermodynamic limit (as the corresponding variance vanishes). We therefore conclude that the BHH eigenvectors in the chaotic regime become ergodic in the eigenbasis of H_{int} in the thermodynamic limit.

Hence, as $\mathcal{N} \to \infty$, the plateau value of $\langle \tilde{D}_1 \rangle$ in Fig. 2 approaches 1, and, although the crossover into the chaotic region becomes more pronounced with larger L, we cannot definitely determine whether it turns into a sharp transition (i.e., a discontinuity of the derivative with respect to η) or remains smooth and differentiable. The transition features a standard scaling behavior [59,60,63,65] in terms of $c_1(\mathcal{N}) \equiv (1 - \langle \tilde{D}_1 \rangle) \ln \mathcal{N}$: For increasing L, c_1 is unbounded in the nonergodic phase (where $\langle \tilde{D}_1 \rangle < 1$, i.e., the eigenstates are generically multifractal), and decreases to converge to a constant value in the chaotic phase if the dominant finite-size correction is $\ln^{-1} \mathcal{N}$. That is indeed the behavior observed numerically (inset of Fig. 2), which confirms that the nonergodic phase for small η persists in the thermodynamic limit. Given the lack of analytical information, we refrain from detailed finite-size scaling analyses on c_1. Nonetheless, close inspection of the tendency of the data locates the transition or crossover, at $\epsilon = 0.5$, in the thermodynamic limit within the region $\eta \in [0.15, 0.2]$ to a reasonable level of confidence. The plateaux's right termination points show no hint of reaching a finite asymptotic value for increasing L, an absence less pronounced for PBCs [70]. Although it is appealing to think that an infinitesimal interaction suffices to induce ergodicity in the thermodynamic limit (as discussed for fermions [76]), and hence that the chaotic phase might have no upper η limit (the point $\eta = \infty$ then being a discontinuity), further investigation is necessary to verify such a hypothesis.

Given the demonstrated quality of RMT predictions, one may naively conclude that, at the level of simple eigenvector observables such as Hilbert space (de)localization captured by GFDs, as L grows the BHH unequivocally assumes universal RMT behavior within its chaotic phase. But a detailed inspection indicates otherwise: Analysis of the full GFD distributions in Fig. 4 reveals that, although the first and second moments approach the GOE values, the distributions become *more distinguishable* from GOE as L increases. The distance between the BHH and GOE distributions is quantified in Fig. 4(c) using the square root of the Kullback-Leibler divergence (relative entropy) [77,78], $\sqrt{KL_q}$, and $d_q(\mathcal{N}) \equiv \delta_q / \sqrt{\mathrm{var}(\tilde{D}_q)}$, where $\delta_q \equiv \langle \tilde{D}_q \rangle_{\mathrm{GOE}} - \langle \tilde{D}_q \rangle$. Both of these measures increase with L for $q = 1, 2, \infty$, demonstrating that, even at the level of the GFDs, the two models depart from each other in a statistically unambiguous way: For $\mathcal{N} \gtrsim 10^6$ ($L \geq 13$, 15, depending on boundary conditions) the typical $\tilde{D}_{1,2}$ lies more than 10σ away from the most probable GOE value. The distance between the GFD distributions provides valuable information on the finite-size corrections for BHH eigenvectors. Since $\mathrm{var}(\tilde{D}_{1,2}) \sim 1/\mathcal{N} \ln^2 \mathcal{N}$, the growth of $d_{1,2}(\mathcal{N})$ with $\mathcal{N}$ entails that $\langle \tilde{D}_{1,2} \rangle$ and $\langle \tilde{D}_{1,2} \rangle_{\mathrm{GOE}}$ differ at terms decaying slower than $1/\sqrt{\mathcal{N}} \ln \mathcal{N}$. A data inspection indicates $d_{1,2}(\mathcal{N}) \sim \sqrt{\mathcal{N}}/\ln \mathcal{N}$ as the most likely behavior for large $\mathcal{N}$, implying that $\langle \tilde{D}_{1,2} \rangle$ bear a $1/\ln^2 \mathcal{N}$ subleading correction [70]. Note that, for nonoverlapping Gaussian distributions of similar width, $\sqrt{KL_q}$ is equivalent to $d_q(\mathcal{N})$. Hence, comparison of these two quantities also provides the distributions' deviation from Gaussianity, as manifestly visible for $q = \infty$.

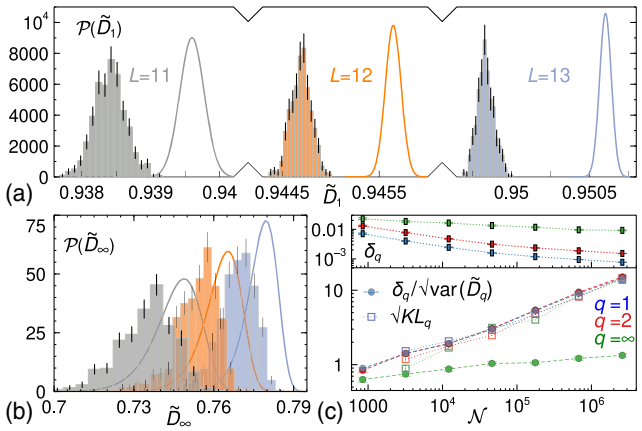

FIG. 4. Evolution of the probability density function of $\tilde{D}_q$ with increasing size $\mathcal{N}$ of the subspace spanned by the $\pi = -1$ eigenstates of H_{int} with HWBCs. Panels (a) and (b) display the distributions of $\tilde{D}_1$ and $\tilde{D}_\infty$, respectively, for the indicated L values. Each histogram comprises 500 eigenstates at $\epsilon = 0.5$ in the chaotic domain (100 eigenstates $\times$ five values of $\eta \in [0.25, 0.38]$). The $\tilde{D}_1$ distribution for $L = 11$ ($L = 12$) is normalized to 4 (2) for better visualization. Solid lines show GOE distributions [70], the distance to which is evaluated in panels (c), via the difference δ_q of the means (upper plot), the renormalized difference $\delta_q / \sqrt{\mathrm{var}(\tilde{D}_q)}$, and the Kullback-Leibler divergence (lower plot).

We finally address the chaotic eigenstates' features' dependence on the expansion basis. Although the GFDs are naturally basis dependent, the eigenstates' ergodic character in the thermodynamic limit suggests some degree of invariance under rotations. An analysis performed in the eigenbasis of H_{tun}, instead of H_{int}, reveals the same qualitative behavior of the energy-resolved $\mathrm{var}(\tilde{D}_q)$ as demonstrated in Fig. 1(d): The GFD fluctuations are strongly suppressed, by several orders of magnitude, and undergo an ever bigger drop for larger system size, within

the same parameter region as observed in the H_{int} basis and in the averaged r statistic. Nonetheless, in the eigenbasis of H_{tun}, there is no clear identification of a $\langle \tilde{D}_q \rangle$ plateau in the chaotic region [70], and the typical GFDs are distant from the GOE values, as shown in the upper panels of Fig. 3. If the GFDs in this basis converge to the ergodic limit, too, this is a much slower process governed by stronger finite-size corrections. Such basis dependence reflects the different dynamics that excited eigenstates of H_{int} or of H_{tun} will exhibit under the BHH unitary evolution: While the first display indications of chaos already in relatively small systems [31,41], the second may be substantially dominated by finite-size and finite-time effects.

We provided an integral view on the chaotic and nonergodic phases of the Bose-Hubbard Hamiltonian, established by an energy-resolved correlation between spectral features and eigenstate structural changes exposed by the typical values and fluctuations of generalized fractal dimensions. Our results suggest that GFD fluctuations are far more sensitive probes of emergent chaotic behavior than the GFDs themselves, and may identify the chaotic phase in any nontrivial basis. In the eigenbasis of the Hamiltonian's interaction part, the chaotic phase eigenvectors become ergodic in the thermodynamic limit, and are remarkably well described by RMT. Yet, in terms of the GFD distributions, their path towards ergodicity turns increasingly more distinguishable from RMT for larger Hilbert spaces, which suggests a statistical handle to discriminate bona fide BHH dynamics in the limit of numerically intractable Hilbert space dimensions. This relates our present results to the field of the certification of distinctive rather than universal features of complex quantum systems [79–82]. Whether this distinct GFD statistics of the BHH with respect to RMT can be traced down to unambiguously unique features of the underlying Hamiltonian, or, alternatively, accommodated by more sophisticated random matrix ensembles [83–85], awaits further scrutiny.

We thank J. D. Urbina for helpful discussions, and acknowledge support by the state of Baden-Württemberg through bwHPC and the German Research Foundation (DFG) through Grants No. INST 40/467-1 FUGG (JUSTUS cluster), No. INST 40/575-1 FUGG (JUSTUS 2 cluster), and No. 402552777. E. G. C. acknowledges support from the Georg H. Endress foundation. A. R. acknowledges support by Universidad de Salamanca through a Grant USAL-C1 (No. 18K145).

*argon@usal.es
†a.buchleitner@physik.uni-freiburg.de

[1] A. J. Lichtenberg and M. A. Lieberman, Regular and Stochastic Motion, *Applied Mathematical Sciences* Vol. 38 (Springer, New York, 1983).
[2] A. M. Ozorio de Almeida, *Hamiltonian Systems: Chaos and Quantization* (Cambridge University Press, Cambridge, England, 1988).
[3] E. Ott, *Chaos in Dynamical Systems* (Cambridge University Press, Cambridge, England, 1993).
[4] A. Pandey, Statistical properties of many-particle spectra: III. Ergodic behaviour in random matrix ensembles, Ann. Phys. (N.Y.) **119**, 170 (1979).
[5] O. Bohigas, Random matrix theories and chaotic dynamics, in *Chaos and Quantum Physics, École d'été de physique théorique des Houches, Session LII* (North Holland, Amsterdam, 1989).
[6] O. Bohigas, M. J. Giannoni, and C. Schmit, Characterization of Chaotic Quantum Spectra and Universality of Level Fluctuation Laws, Phys. Rev. Lett. **52**, 1 (1984).
[7] M. V. Berry, Regular and irregular semiclassical wavefunctions, J. Phys. A **10**, 2083 (1977).
[8] D. Delande and J. C. Gay, Quantum Chaos and Statistical Properties of Energy Levels: Numerical Study of the Hydrogen Atom in a Magnetic Field, Phys. Rev. Lett. **57**, 2006 (1986).
[9] I. M. Khaymovich, M. Haque, and P. A. McClarty, Eigenstate Thermalization, Random Matrix Theory, and Behemoths, Phys. Rev. Lett. **122**, 070601 (2019).
[10] G. De Tomasi and I. M. Khaymovich, Multifractality Meets Entanglement: Relation for Nonergodic Extended States, Phys. Rev. Lett. **124**, 200602 (2020).
[11] F. M. Izrailev, Simple models of quantum chaos: Spectrum and eigenfunctions, Phys. Rep. **196**, 299 (1990).
[12] T. Geisel, G. Radons, and J. Rubner, Kolmogorov-Arnol'd-Moser Barriers in the Quantum Dynamics of Chaotic Systems, Phys. Rev. Lett. **57**, 2883 (1986).
[13] O. Bohigas, S. Tomsovic, and D. Ullmo, Manifestations of classical phase space structures in quantum mechanics, Phys. Rep. **223**, 43 (1993).
[14] A. Buchleitner, D. Delande, J. Zakrzewski, R. N. Mantegna, M. Arndt, and H. Walther, Multiple Time Scales in the Microwave Ionization of Rydberg Atoms, Phys. Rev. Lett. **75**, 3818 (1995).
[15] R. Ketzmerick, L. Hufnagel, F. Steinbach, and M. Weiss, New Class of Eigenstates in Generic Hamiltonian Systems, Phys. Rev. Lett. **85**, 1214 (2000).
[16] M. Hiller, T. Kottos, and T. Geisel, Complexity in parametric Bose-Hubbard Hamiltonians and structural analysis of eigenstates, Phys. Rev. A **73**, 061604(R) (2006).
[17] A. A. Michailidis, C. J. Turner, Z. Papić, D. A. Abanin, and M. Serbyn, Slow Quantum Thermalization and Many-Body Revivals from Mixed Phase Space, Phys. Rev. X **10**, 011055 (2020).
[18] H. A. Weidenmüller and G. E. Mitchell, Random matrices and chaos in nuclear physics: Nuclear structure, Rev. Mod. Phys. **81**, 539 (2009).
[19] A. Bäcker, M. Haque, and I. M. Khaymovich, Multifractal dimensions for random matrices, chaotic quantum maps, and many-body systems, Phys. Rev. E **100**, 032117 (2019).
[20] A. R. R. Carvalho and A. Buchleitner, Web-Assisted Tunneling In The Kicked Harmonic Oscillator, Phys. Rev. Lett. **93**, 204101 (2004).
[21] T. Gericke, P. Würtz, D. Reitz, T. Langen, and H. Ott, High-resolution scanning electron microscopy of an ultracold quantum gas, Nat. Phys. **4**, 949 (2008).

[22] M. Karski, L. Förster, J. M. Choi, W. Alt, A. Widera, and D. Meschede, Nearest-Neighbor Detection of Atoms in a 1D Optical Lattice by Fluorescence Imaging, Phys. Rev. Lett. **102**, 053001 (2009).
[23] N. Gemelke, X. Zhang, C. L. Hung, and C. Chin, In situ observation of incompressible Mott-insulating domains in ultracold atomic gases, Nature (London) **460**, 995 (2009).
[24] J. F. Sherson, C. Weitenberg, M. Endres, M. Cheneau, I. Bloch, and S. Kuhr, Single-atom-resolved fluorescence imaging of an atomic Mott insulator, Nature (London) **467**, 68 (2010).
[25] W. S. Bakr, A. Peng, M. E. Tai, R. Ma, J. Simon, J. I. Gillen, S. Fölling, L. Pollet, and M. Greiner, Probing the superfluid-to-Mott insulator transition at the single-atom level, Science **329**, 547 (2010).
[26] F. Meinert, M. J. Mark, K. Lauber, A. J. Daley, and H.-C. Nägerl, Floquet Engineering of Correlated Tunneling in the Bose-Hubbard Model with Ultracold Atoms, Phys. Rev. Lett. **116**, 205301 (2016).
[27] J. P. Ronzheimer, M. Schreiber, S. Braun, S. S. Hodgman, S. Langer, I. P. McCulloch, F. Heidrich-Meisner, I. Bloch, and U. Schneider, Expansion Dynamics of Interacting Bosons in Homogeneous Lattices in One and Two Dimensions, Phys. Rev. Lett. **110**, 205301 (2013).
[28] F. Meinert, M. J. Mark, E. Kirilov, K. Lauber, P. Weinmann, M. Gröbner, and H.-C. Nägerl, Interaction-Induced Quantum Phase Revivals and Evidence for the Transition to the Quantum Chaotic Regime in 1D Atomic Bloch Oscillations, Phys. Rev. Lett. **112**, 193003 (2014).
[29] P. M. Preiss, R. Ma, M. E. Tai, A. Lukin, M. Rispoli, P. Zupancic, Y. Lahini, R. Islam, and M. Greiner, Strongly correlated quantum walks in optical lattices, Science **347**, 1229 (2015).
[30] R. Islam, R. Ma, P. M. Preiss, M. E. Tai, A. Lukin, M. Rispoli, and M. Greiner, Measuring entanglement entropy in a quantum many-body system, Nature (London) **528**, 77 (2015).
[31] A. M. Kaufman, M. E. Tai, A. Lukin, M. Rispoli, R. Schittko, P. M. Preiss, and M. Greiner, Quantum thermalization through entanglement in an isolated many-body system, Science **353**, 794 (2016).
[32] A. R. Kolovsky and A. Buchleitner, Quantum chaos in the Bose-Hubbard model, Europhys. Lett. **68**, 632 (2004).
[33] C. Kollath, G. Roux, G. Biroli, and A. M. Läuchli, Statistical properties of the spectrum of the extended Bose-Hubbard model, J. Stat. Mech. (2010) P08011.
[34] R. Dubertrand and S. Müller, Spectral statistics of chaotic many-body systems, New J. Phys. **18**, 033009 (2016).
[35] D. Fischer, D. Hoffmann, and S. Wimberger, Spectral analysis of two-dimensional Bose-Hubbard models, Phys. Rev. A **93**, 043620 (2016).
[36] W. Beugeling, R. Moessner, and M. Haque, Finite-size scaling of eigenstate thermalization, Phys. Rev. E **89**, 042112 (2014).
[37] W. Beugeling, R. Moessner, and M. Haque, Off-diagonal matrix elements of local operators in many-body quantum systems, Phys. Rev. E **91**, 012144 (2015).
[38] W. Beugeling, A. Andreanov, and M. Haque, Global characteristics of all eigenstates of local many-body Hamiltonians: Participation ratio and entanglement entropy, J. Stat. Mech. (2015) P02002.
[39] W. Beugeling, A. Bäcker, R. Moessner, and M. Haque, Statistical properties of eigenstate amplitudes in complex quantum systems, Phys. Rev. E **98**, 022204 (2018).
[40] A. Buchleitner and A. R. Kolovsky, Interaction-Induced Decoherence of Atomic Bloch Oscillations, Phys. Rev. Lett. **91**, 253002 (2003).
[41] S. Sorg, L. Vidmar, L. Pollet, and F. Heidrich-Meisner, Relaxation and thermalization in the one-dimensional Bose-Hubbard model: A case study for the interaction quantum quench from the atomic limit, Phys. Rev. A **90**, 033606 (2014).
[42] C. Kollath, A. M. Läuchli, and E. Altman, Quench Dynamics and Nonequilibrium Phase Diagram of the Bose-Hubbard Model, Phys. Rev. Lett. **98**, 180601 (2007).
[43] G. Roux, Finite-size effects in global quantum quenches: Examples from free bosons in an harmonic trap and the one-dimensional Bose-Hubbard model, Phys. Rev. A **81**, 053604 (2010).
[44] G. Biroli, C. Kollath, and A. M. Läuchli, Effect of Rare Fluctuations on the Thermalization of Isolated Quantum Systems, Phys. Rev. Lett. **105**, 250401 (2010).
[45] M. Lewenstein, A. Sanpera, V. Ahufinger, B. Damski, A. Sen, and U. Sen, Ultracold atomic gases in optical lattices: Mimicking condensed matter physics and beyond, Adv. Phys. **56**, 243 (2007).
[46] M. A. Cazalilla, R. Citro, T. Giamarchi, E. Orignac, and M. Rigol, One dimensional bosons: From condensed matter systems to ultracold gases, Rev. Mod. Phys. **83**, 1405 (2011).
[47] K. V. Krutitsky, Ultracold bosons with short-range interaction in regular optical lattices, Phys. Rep. **607**, 1 (2016).
[48] M. Hiller, T. Kottos, and T. Geisel, Wave-packet dynamics in energy space of a chaotic trimeric Bose-Hubbard system, Phys. Rev. A **79**, 023621 (2009).
[49] F. Pietracaprina, N. Macé, D. J. Luitz, and F. Alet, Shift-invert diagonalization of large many-body localizing spin chains, SciPost Phys. **5**, 045 (2018).
[50] S. Balay, S. Abhyankar, M. F. Adams, J. Brown, P. Brune, K. Buschelman, L. Dalcin, A. Dener, V. Eijkhout, W. D. Gropp, D. Karpeyev, D. Kaushik, M. G. Knepley, D. A. May, L. C. McInnes, R. T. Mills, T. Munson, K. Rupp, P. Sanan, B. F. Smith, S. Zampini, H. Zhang, and H. Zhang, PETSc Users Manual, Technical Report No. ANL-95/11—Revision 3.13 (Argonne National Laboratory, 2020).
[51] V. Hernandez, J. E. Roman, and V. Vidal, SLEPc: A scalable and flexible toolkit for the solution of eigenvalue problems, ACM Trans. Math. Softw. **31**, 351 (2005).
[52] V. Oganesyan and D. A. Huse, Localization of interacting fermions at high temperature, Phys. Rev. B **75**, 155111 (2007).
[53] Y. Y. Atas, E. Bogomolny, O. Giraud, and G. Roux, Distribution of the Ratio of Consecutive Level Spacings in Random Matrix Ensembles, Phys. Rev. Lett. **110**, 084101 (2013).
[54] J.-M. Stéphan, S. Furukawa, G. Misguich, and V. Pasquier, Shannon and entanglement entropies of one- and two-dimensional critical wave functions, Phys. Rev. B **80**, 184421 (2009).

[55] J.-M. Stéphan, G. Misguich, and V. Pasquier, Rényi entropy of a line in two-dimensional Ising models, Phys. Rev. B **82**, 125455 (2010).

[56] J.-M. Stéphan, G. Misguich, and V. Pasquier, Phase transition in the Rényi-Shannon entropy of Luttinger liquids, Phys. Rev. B **84**, 195128 (2011).

[57] Y. Y. Atas and E. Bogomolny, Multifractality of eigenfunctions in spin chains, Phys. Rev. E **86**, 021104 (2012).

[58] Y. Y. Atas and E. Bogomolny, Calculation of multi-fractal dimensions in spin chains, Phil. Trans. R. Soc. A **372**, 20120520 (2014).

[59] D. J. Luitz, F. Alet, and N. Laflorencie, Universal Behavior Beyond Multifractality in Quantum Many-Body Systems., Phys. Rev. Lett. **112**, 057203 (2014).

[60] D. J. Luitz, N. Laflorencie, and F. Alet, Many-body localization edge in the random-field Heisenberg chain, Phys. Rev. B **91**, 081103(R) (2015).

[61] G. Misguich, V. Pasquier, and M. Oshikawa, Finite-size scaling of the Shannon-Rényi entropy in two-dimensional systems with spontaneously broken continuous symmetry, Phys. Rev. B **95**, 195161 (2017).

[62] J. Lindinger, A. Buchleitner, and A. Rodríguez, Many-Body Multifractality throughout Bosonic Superfluid and Mott Insulator Phases, Phys. Rev. Lett. **122**, 106603 (2019).

[63] N. Macé, F. Alet, and N. Laflorencie, Multifractal Scalings Across the Many-Body Localization Transition, Phys. Rev. Lett. **123**, 180601 (2019).

[64] D. J. Luitz, I. Khaymovich, and Y. Bar Lev, Multifractality and its role in anomalous transport in the disordered XXZ spin-chain, SciPost Phys. Core **2**, 006 (2020).

[65] A. Rodriguez, L. J. Vasquez, K. Slevin, and R. A. Römer, Multifractal finite-size scaling and universality at the Anderson transition, Phys. Rev. B **84**, 134209 (2011).

[66] While exponential localization implies vanishing D_q for all $q > 0$, nonexponentially localized states may exhibit $D_q \neq 0$ for some $q < 1$, such as those in a generalized Rosenzweig-Porter model [67].

[67] V. E. Kravtsov, I. M. Khaymovich, E. Cuevas, and M. Amini, A random matrix model with localization and ergodic transitions, New J. Phys. **17**, 122002 (2015).

[68] A. Mirlin, Statistics of energy levels and eigenfunctions in disordered systems, Phys. Rep. **326**, 259 (2000).

[69] L. Pausch (to be published).

[70] See Supplemental Material http://link.aps.org/supplemental/10.1103/PhysRevLett.126.150601 for further information and where, additionally, Refs. [71–73] are cited.

[71] Y. V. Fyodorov and O. Giraud, High values of disorder-generated multifractals and logarithmically correlated processes, Chaos Solitons Fractals **74**, 15 (2015).

[72] F. W. J. Olver, A. B. Olde Daalhuis, D. W. Lozier, B. I. Schneider, R. F. Boisvert, C. W. Clark, B. R. Miller, B. V. Saunders, H. S. Cohl, and M. A. McClain, NIST Digital Library of Mathematical Functions, http://dlmf.nist.gov/, Release 1.0.27 of 2020-06-15.

[73] O. Giraud, N. Macé, E. Vernier, and F. Alet, Probing symmetries of quantum many-body systems through gap ratio statistics, arXiv:2008.11173.

[74] F. Haake, S. Gnutzmann, and M. Kuś, *Quantum Signatures of Chaos*, Springer Series in Synergetics (Springer International Publishing, Cham, 2018).

[75] A. Lakshminarayan, S. Tomsovic, O. Bohigas, and S. N. Majumdar, Extreme Statistics of Complex Random and Quantum Chaotic States, Phys. Rev. Lett. **100**, 044103 (2008).

[76] C. Neuenhahn and F. Marquardt, Thermalization of interacting fermions and delocalization in Fock space, Phys. Rev. E **85**, 060101(R) (2012).

[77] S. Kullback and R. A. Leibler, On information and sufficiency, Ann. Math. Stat. **22**, 79 (1951).

[78] T. M. Cover and J. A. Thomas, *Elements of Information Theory* (John Wiley & Sons, Hoboken, 2006).

[79] M. C. Tichy, M. Tiersch, F. de Melo, F. Mintert, and A. Buchleitner, Zero-Transmission Law for Multiport Beam Splitters, Phys. Rev. Lett. **104**, 220405 (2010).

[80] L. Aolita, C. Gogolin, M. Kliesch, and J. Eisert, Reliable quantum certification of photonic state preparations, Nat. Commun. **6**, 8498 (2015).

[81] T. Giordani, F. Flamini, M. Pompili, N. Viggianiello, N. Spagnolo, A. Crespi, R. Osellame, N. Wiebe, M. Walschaers, A. Buchleitner, and F. Sciarrino, Experimental statistical signature of many-body quantum interference, Nat. Photonics **12**, 173 (2018).

[82] T. V. Zache, T. Schweigler, S. Erne, J. Schmiedmayer, and J. Berges, Extracting the Field Theory Description of a Quantum Many-Body System from Experimental Data, Phys. Rev. X **10**, 011020 (2020).

[83] K. Mon and J. French, Statistical properties of many-particle spectra, Ann. Phys. (N.Y.). **95**, 90 (1975).

[84] L. Benet and H. A. Weidenmüller, Review of the k -body embedded ensembles of Gaussian random matrices, J. Phys. A **36**, 3569 (2003).

[85] N. D. Chavda and V. K. B. Kota, Localization-delocalization transitions in bosonic random matrix ensembles, Ann. Phys. (Amsterdam) **529**, 1600287 (2017).